Antiprotozoal Activities of Heterocyclic-Substituted Xanthones from the Marine-Derived Fungus *Chaetomium* sp.

Alexander Pontius,[†] Anja Krick,[†] Stefan Kehraus,[†] Reto Brun,[‡] and Gabriele M. König*,[†]

Institute for Pharmaceutical Biology, University of Bonn, Nussallee 6, 53115 Bonn, Germany, and Swiss Tropical Institute, Socinstrasse 57, 4002 Basel, Switzerland

Received May 14, 2008

Investigations of the marine-derived fungus *Chaetomium* sp. led to the isolation of the new natural products chaetoxanthones A, B, and C (**1**−**3**). Compounds **1** and **2** are substituted with a dioxane/tetrahydropyran moiety rarely found in natural products. Compound **3** was identified as a chlorinated xanthone substituted with a tetrahydropyran ring. The configurational analysis of these compounds employed CD spectroscopy, modified Mosher's method, and selective NOE gradient measurements. Compound **2** showed selective activity against *Plasmodium falciparum* with an IC_{50} value of 0.5 μg/mL without being cytotoxic toward cultured eukaryotic cells. Compound **3** displayed a moderate activity against *Trypanosoma cruzi* with an IC_{50} value of 1.5 μg/mL.

Xanthones represent a structurally diverse group of natural products with a broad range of biological activities.[1] Several xanthones derived from higher plants, lichens, and fungi, as well as synthetic xanthone derivatives, were found to be promising compounds to treat plasmodial organisms.[2−4]

More than 3 billion people are affected by protozoan diseases such as malaria, leishmaniasis, and Chagas' disease. About 500 million become severely ill with malaria every year, and at least 1 million, in particular children, die from the effects of the disease.[5,6] Because of an increasing resistance against established and widely used drugs such as chloroquine and sulfadoxine/pyrimethamine, the discovery of novel classes of active substances or the use of resistance-reversing agents such as 9*H*-xanthene derivatives is extremely important.[7,8]

Recently published xanthones revealed promising antiprotozoal activities but also showed pronounced cytotoxicity, making them problematic for pharmaceutical use.[9] The mode of action of xanthones toward *Plasmodium* parasites was investigated in detail, and they are considered to inhibit heme polymerization. Thus, the detoxification of harmful hematin decreases and provokes the death of the parasitic cells.[13,14] The substitution pattern of the xanthone basic skeleton has an enormous influence on the activity of the molecules, and SAR studies were performed for a number of xanthones.[10−12]

Results and Discussion

Investigations of the marine-derived fungus *Chaetomium* sp. yielded three new xanthones with unusual and rare structural features for this structural class of natural products. Compound **2** was found to possess *in vitro* antimalarial activity against *Plasmodium falciparum* with an IC_{50} value of 0.5 μg/mL, while compound **3** inhibited the growth of *Trypanosoma cruzi*, the causative pathogen of Chagas' disease, with an IC_{50} value of 1.5 μg/mL. The new xanthones (**2**, **3**) showed selective effects toward the protozoal strains *Plasmodium falciparum* and *Trypanosoma cruzi* with only low cytotoxicity for **3** (IC_{50} = 47 μg/mL) and no observed cytotoxic effects for **2** up to 90 μg/mL.

The molecular formula of compound **1** was deduced by accurate mass measurement (HREIMS) to be $C_{20}H_{18}O_7$, implying 12 degrees of unsaturation. UV-absorption maxima at λ_{max} 245 and 323 nm suggested an extended mesomerically stabilized aromatic system.

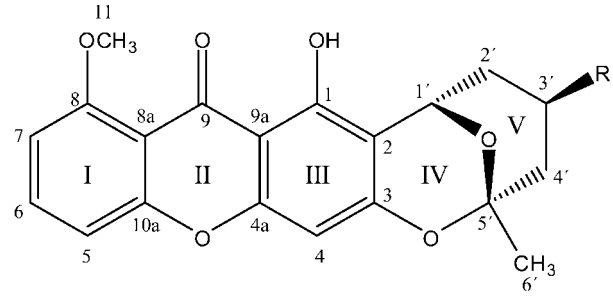

1 R = OH (1′*S*, 3′*R*, 5′*S*)

2 R = H (as a racemic mixture)

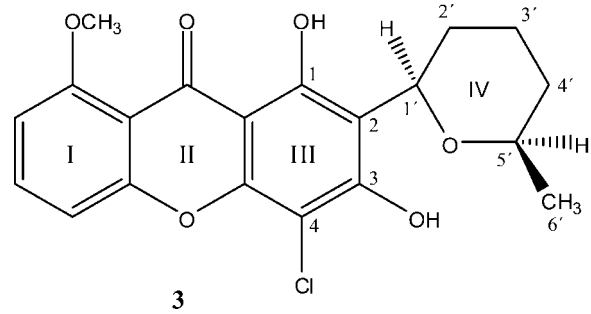

3

The ^{1}H NMR spectrum contained characteristic signals of a chelated hydroxyl group (δ_H 13.77, OH-1), three vicinal aromatic protons (δ_H 7.69, H-6; δ_H 7.00, H-5; δ_H 6.95, H-7), a single aromatic proton (δ_H 6.23, H-4), two downfield shifted aliphatic methine groups (δ_H 5.28, H-1′; δ_H 3.87, H-3′), and the signal for a methoxyl group (δ_H 3.96, H_3-11). Furthermore, signals for two aliphatic methylene groups (δ_H 2.20/1.80, H_2-2′; δ_H 2.37/1.69, H_2-4′) and a methyl group were found (δ_H 1.57, H_3-6′). Due to the molecular formula and the 17 protons evident from the ^{1}H NMR spectrum, one proton had to be present most probably as an aliphatic hydroxyl group. From the ^{13}C NMR spectrum, which contained a signal for a carbonyl group (δ_C 181.9, C-9) together with 12 aromatic carbon resonances, a xanthone framework, consisting of two outer benzene rings and a central γ-pyrone moiety, was suggested. Benzene ring I had three *ortho*-positioned aromatic protons, with H-6 due to its triplet ^{1}H NMR resonance signal in a middle position. ^{1}H−^{13}C HMBC NMR measurements clarified the substitution pattern of ring I (see Figure S1). The methoxyl proton signal (CH_3-11) possessed HMBC cross-peaks to C-7 and C-8, indicating its position at C-8. HMBC correlations of H-6 to C-10a, H-7 to C-8a, and H-5 to C-9

* To whom correspondence should be addressed. Tel: +49228733747. Fax: +49228733250. E-mail: g.koenig@uni-bonn.de.
[†] University of Bonn.
[‡] Swiss Tropical Institute.

10.1021/np800294q CCC: $40.75
Published on Web 08/07/2008

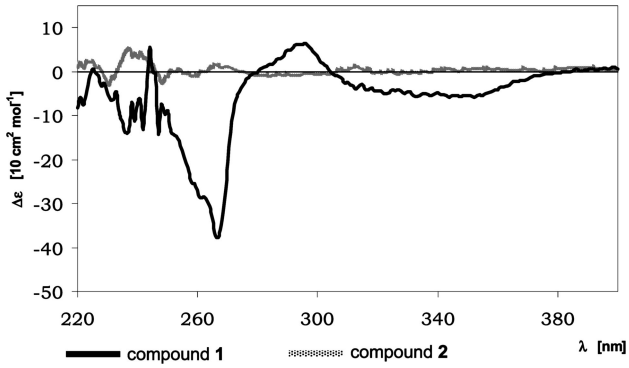

Figure 1. CD spectra of **1** and **2** recorded in acetonitrile.

proved the chromone substructure of the framework consisting of the rings I and II. Ring III had only one aromatic proton and was otherwise fully substituted. The hydrogen-bonding hydroxyl group was identified as part of a phenylogous acid and had to be positioned at C-1. Long-range HMBC couplings between the single aromatic proton H-4 and C-4a, C-9a, and C-9 evidenced the *para* position of H-4 and OH-1. The ^{1}H−^{1}H-COSY experiment revealed an aliphatic spin system from H-1′ through H$_2$-4′, including the oxygen-bearing methine groups CH-1′ and CH-3′. This fragment was part of a tetrahydropyran moiety (ring V) that was connected to a dioxane ring (ring IV) via the single oxygenated carbon C-1′ and the double oxygenated carbon C-5′. These two heterocycles were deduced from HMBC couplings of H$_3$-6′ to C-1′ and C-5′ as well as H$_2$-4′ to C-5′. HMBC correlations of H-1′ to C-3, Hβ-2′ to C-2, and H$_3$-6′ to C-3 proved the connection of the tetrahydropyran/dioxane moiety via the benzene III carbons C-2 and C-3 to the xanthone framework.

The geometry of the molecule was considered to have the dioxane ring arranged coplanar to the xanthone moiety with the tetrahydropyran ring in vertical orientation and in nearly ideal chair conformation. This architecture of the outer rings was established from the magnitude of ^{1}H−^{1}H coupling constants. The resonance of H-1′ appeared as a doublet of doublets with $J_{1',\,2\alpha'} = 1.8$ Hz and $J_{1',\,2\beta'} = 4.4$ Hz, proving the equatorial position of proton H-1′. Consequently, CH$_3$-6′ must also be oriented equatorially and on the same side of the molecule as H-1′ (see Figure S2).[15] The ^{1}H NMR signal of proton H-3′ revealed medium ($J_{3',\,2\alpha'} = 5.4$ Hz, $J_{3',\,4\alpha'} = 5.4$ Hz) and large coupling constants ($J_{3',\,2\beta'} = 10.8$ Hz, $J_{3',\,4\beta'} = 10.8$ Hz) with protons of each vicinal methylene group CH$_2$-2′ and CH$_2$-4′, respectively. Hence, proton H-3′ is in an axial position with an equatorially arranged hydroxyl group at C-3′.

A modified Mosher's method was applied to determine the absolute configuration at C-3′. The calculated differences in chemical shifts [δ of protons in the (*R*)-MPA-ester − δ of the corresponding protons in the (*S*)-MPA ester] led to the assignment of the *R* absolute configuration for C-3′ (see Figure S3, Table S1).[16] To clarify the configuration at C-1′ and C-5′, two energy-minimized structures were modeled with 1′*R*, 3′*R*, 5′*R* configuration (model *a*) and with 1′*S*, 3′*R*, 5′*S* configuration (model *b*) (see Figure S4). Model *a* did not yield torsion angles that were in agreement with the ^{1}H−^{1}H coupling constants for the protons H-1′ and H$_2$-2′ and excluded a chair conformation for the tetrahydropyran ring. Additionally, the spacial proximity of H-3′, H-1′, and H$_3$-6′ (model *a*) would be expected to result in clear NOE correlations, which were, however, not detected. Taking the results of all NMR experiments into account, model *b* provided the best fit for the structure of compound **1**, which thus has a 1′*S*, 3′*R*, 5′*S* absolute configuration. We propose the trivial name chaetoxanthone A for compound **1**.

Compound **2** was found to have the molecular formula C$_{20}$H$_{18}$O$_6$ as deduced by HREIMS and compared to compound **1** lacked an oxygen atom. Both compounds showed very similar ^{13}C NMR data, but differed concerning the low-field ^{13}C NMR signals for the tetrahydropyran carbons C-2′, C-3′, and C-4′. Taking into account the ^{13}C NMR resonance for an unsubstituted CH$_2$− group (δ_H 1.56, H$_2$-3′) within **2** instead of a signal for an aliphatic oxygen-bearing methine group (δ_H 3.87, H-3′) as in **1**, compound **2** was concluded to be lacking the C-3′ hydroxyl group. While the CD curve of **1** revealed a positive Cotton effect at 296 nm followed by a negative one at 267 nm, no significant Cotton effects in the spectrum of **2** were visible (see Figure 1). Since no specific optical rotation could be determined for **2**, it is most probably a mixture of enantiomers in a ratio of about 1:1. For compound **2** we propose the trivial name chaetoxanthone B.

The molecular formula of compound **3** was analyzed by HREIMS to be C$_{20}$H$_{19}$ClO$_6$. The UV spectrum with the maxima at 265 and 323 nm suggested a xanthone-type chromophore. Comparison of the 1D and 2D NMR spectra of **3** with those of **1** and **2** revealed that they shared the structure of rings I and II; however, significant differences were obvious for xanthone ring III and the outer ring IV. Apart from ^{1}H NMR signals for H-5, H-6, and H-7 no further aromatic proton was depicted, but an additional downfield shifted signal for a hydroxyl group at δ_H 10.52 (OH-3) was found. Furthermore, the characteristic ^{13}C NMR signal for a double oxygenated quaternary carbon (C-5′) as present in **1** and **2** was missing, and instead a signal for an oxygen-bearing sp^3-hybridized methine group at δ_H 76.0 (CH-5′) appeared. The ^{1}H−^{1}H-COSY experiment allowed the assignment of an aliphatic spin system from H-1′ through H$_3$-6′, including both oxygenated methine groups CH-1′ and CH-5′. The HMBC experiment exhibited cross-peaks of H-1′ to C-5′, indicating the presence of a methyl-substituted tetrahydropyran moiety (ring IV). The *peri* position of the hydrogen-bonding hydroxyl group (δ_H 13.62, OH-1) adjacent to the xanthone carbonyl group was sustained by correlations of OH-1 to the carbons C-1, C-2, C-3, C-9a, and C-9. The second hydroxyl group (δ_H 10.52, OH-3) was considered to be at C-3 because of its HMBC cross-peaks to C-2, C-3, C-4, and C-4a. Subsequently, HMBC correlations of H-1′ to C-1, C-2, and C-3 indicated the tetrahydropyran moiety at C-2 in the *ortho* position to the hydroxyl groups. On the basis of the elemental composition, the remaining substituent at C-4 was the chlorine atom, completing ring III within compound **3**. Selective NOE measurements were undertaken to establish the relative configuration of compound **3**. The significant NOE enhancement observed for the ^{1}H NMR resonance of H-5′ upon irradiation of the H-1′ resonance, and vice versa, indicated that both methine protons were located on the same side of the molecule and in the axial position on the six-membered ring IV (Figure S5). A further clear NOE correlation between the equatorially bonded methyl group CH$_3$-6′ and the hydroxyl group OH-3 sustained this arrangement. With regard to the NOE experiments, molecular modeling calculation of compound **3** resulted in a minimum energy structure where the tetrahydropyran derivative adopted the boat conformation. The relative configuration of compound **3** was deduced as 1′*R*, 5′*R* or 1′*S*, 5′*S*, respectively, and we propose the trivial name chaetoxanthone C.

The new xanthones were tested in a series of *in vitro* bioassays for their antiprotozoal activities and cytotoxic potency. Compound **2** exhibited selective antiprotozoal activity toward *Plasmodium falciparum* with an IC$_{50}$ value of 0.5 μg/mL and no cytotoxic effects toward L6-cells (IC$_{50}$ >90 μg/mL) and 35 tumor cell lines (mean IC$_{50}$ >10 μg/mL). Compound **3** was found to be moderately active against *Trypanosoma cruzi* with an IC$_{50}$ value of 1.5 μg/mL without having considerable cytotoxic effects on L6-cells (IC$_{50}$ = 46.7 μg/mL).

The characteristic structural feature for compounds **1**−**3** is the presence of unusual heterocyclic rings on the xanthone framework. To date, xanthones substituted with a dioxane/tetrahydropyran moiety were found only in the natural products averufin and nidurufin, as well as in derivatives and related synthetic products

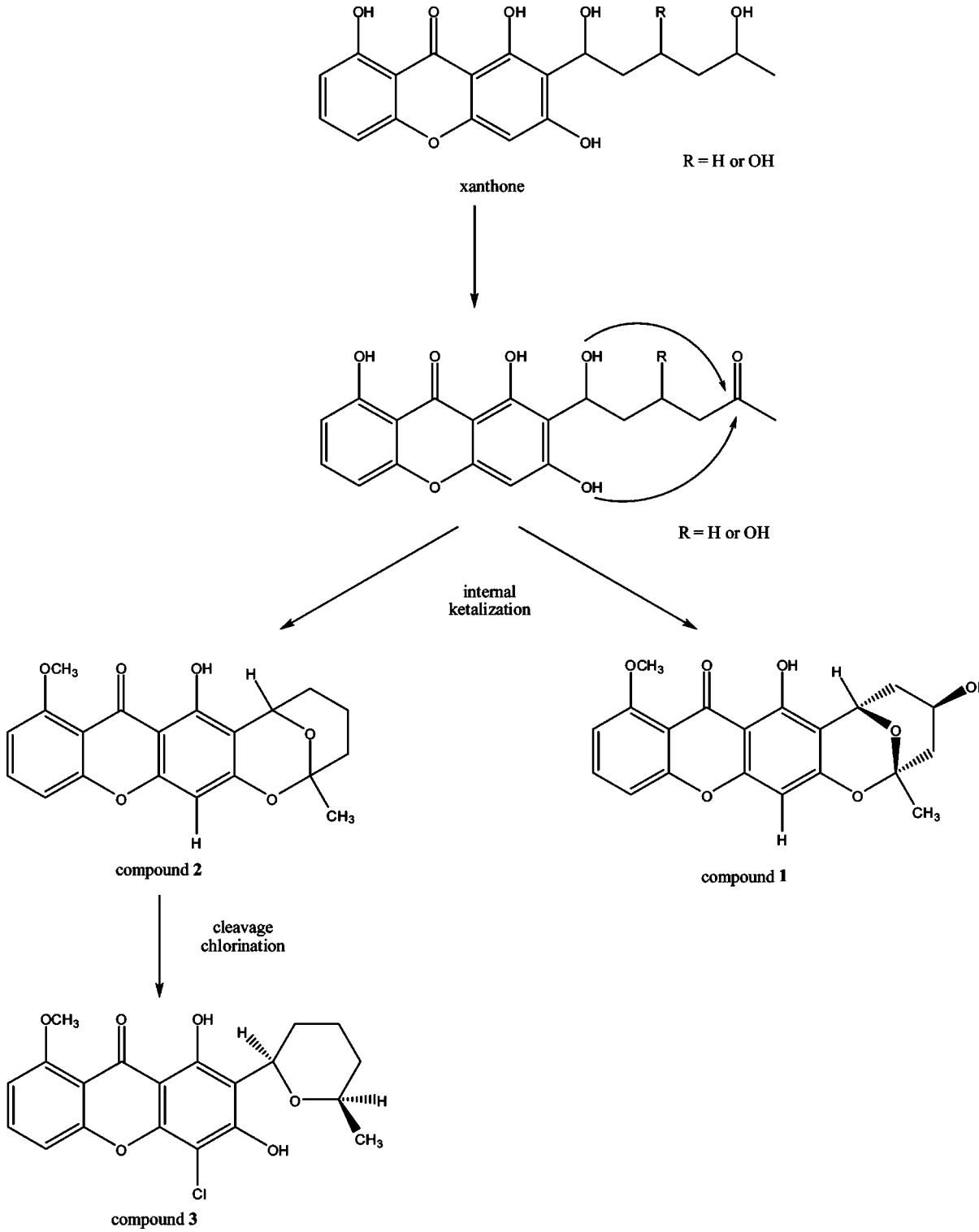

Figure 2. Proposed biosynthetic relationship of chaetoxanthones.

of them (see Figure S10).[17−19] The decaketide-based biosynthesis of this type of xanthones was suggested to proceed via the anthraquinoid precursors averantin and norsolorinic acid, which also play a role in the well-investigated aflatoxin pathway.[20,21] The hydroxyl groups at C-1′ of the side chain and at C-3 of the xanthone essentially undergo an internal ketalization with the carbonyl group C-5′ forming the bicyclic moiety, which is finally cleaved to the methyl-substituted tetrahydropyran ring (IV) within **3** (see Figures 2, S6). Chlorine substitution of xanthones was found in a wide range of lichen-derived metabolites.[22] The occurrence of chlorinated xanthones in fungi as elucidated for **3** is, however, described for only two metabolites, i.e., 4-chloropinselin and chloroisosulochrin dehydrate (see Figure S10).[23,24]

Among the isolated xanthones, compound **2** achieved the best *in vitro* antiplasmodial activity (IC_{50} = 0.5 μg/mL, *Plasmodium falciparum*) with an at least 7.5-fold enhanced potency compared to the other tested protozoans. Our work confirms the xanthone nucleus as a suitable pharmacophore for antiplasmodial activity, and substitution of this framework clearly influences the biological effect. Compound **2** did not reach the high antiplasmodial potency of some reported polyhydroxyxanthones[4] or alkylamino-substituted xanthones[11] with IC_{50} values below 0.1 μg/mL, but was more active

Table 1. 1D and 2D NMR Spectroscopic Data for Chaetoxanthone A (**1**)

atom no.	δ_C[a,c,f]	δ_H[a,c] (mult., *J* in Hz)	COSY[a,d]	HMBC[a,e]	sel. NOE[b,d]
1	158.6 (C)				
2	106.3 (C)				
3	160.3 (C)				
4	93.3 (CH)	6.23 (s)		2, 3, 4a, 9, 9a	
4a	156.3 (C)				
5	110.2 (CH)	7.00 (d, 8.5)	6	7, 8a, 9, 10a	
6	136.7 (CH)	7.69 (t, 8.5)	5, 7	5, 7, 8, 8a, 10a	
7	107.1 (CH)	6.95 (d, 8.5)	6	5, 8, 8a	
8	161.7 (C)				
8a	111.4 (C)				
9	181.9 (C)				
9a	103.7 (C)				
10a	158.5 (C)				
11	56.6 (CH_3)	3.96 (s)		7, 8	
1′	67.4 (CH)	5.28 (dd, 1.8,4.4)	2′	2, 3, 2′, 3′, 5′	2′*β*
2′	38.4 (CH_2)	2.20 (H*α* ddt, 12.6, 5.4, 1.8)	1′, 3′	3′	
		1.80 (H*β* ddd, 4.4, 10.8, 12.6)	1′, 3′	2, 1′, 3′, 5′	
3′	62.2 (CH)	3.87 (tt, 5.4, 10.8)	2′, 4′	2′, 4′	4′α
4′	46.5 (CH_2)	2.37 (H*α* ddd, 1.5,5.4, 13.2)	3′	3′, 5′	
		1.69 (H*β* dd, 10.8, 13.2)	3′	3′, 5′	
5′	103.1 (C)				
6′	28.2 (CH_3)	1.57 (brs)		3, 1′, 3′,5′	4′*β*
OH-1		13.77 (s)		1, 2, 9a	

[a] Acetone-d_6, 300/75.5 MHz. [b] Acetone-d_6, 500/125.7 MHz. [c] Assignments are based on extensive 1D and 2D NMR measurements (HMBC, HSQC, COSY). [d] Numbers refer to proton resonances. [e] Numbers refer to carbon resonances. [f] Implied multiplicities determined by DEPT.

Table 2. 1D and 2D NMR Spectroscopic Data for Chaetoxanthone B (**2**)

atom no.	δ_C[a,b,e]	δ_H[a,b] (mult., *J* in Hz)	COSY[a,c]	HMBC[a,d]
1	157.8 (C)			
2	105.2 (C)			
3	160.6 (C)			
4	92.5 (CH)	6.18 (s)		2, 3, 4a, 9, 9a
4a	155.4 (C)			
5	109.7 (CH)	6.86 (d, 8.4)	6	7, 8a, 9, 10a
6	135.1 (CH)	7.45 (t, 8.4)	5, 7	7, 8, 8a, 10a
7	105.4 (CH)	6.66 (d, 8.4)	6	5, 8, 8a, 9, 10a
8	160.4 (C)			
8a	110.7 (C)			
9	181.4 (C)			
9a	103.1 (C)			
10a	157.7 (C)			
11	56.4 (CH_3)	3.92 (s)		7, 8
1′	67.0 (CH)	5.27 (m)	2′	1, 2, 3, 3′, 5′
2′	27.7 (CH_2)	1.94 (H*α* m)	1′, 3′	4′
		1.77 (H*β* m)	1′, 3′	4′
3′	15.8 (CH_2)	1.56 (m)	2′, 4′	4′
4′	35.7 (CH_2)	1.94 (H*α* m)	3′	2′, 3′, 5′
		1.77 (H*β* m)	3′	2′, 3′, 5′
5′	100.8 (C)			
6′	27.9 (CH_3)	1.49 (s)		3, 1′, 3′, 4′, 5′
OH-1		13.34 (s)		1, 2, 3, 9a

[a] Chloroform-d_1, 300/75.5 MHz. [b] Assignments are based on extensive 1D and 2D NMR measurements (HMBC, HSQC, COSY). [c] Numbers refer to proton resonances. [d] Numbers refer to carbon resonances. [e] Implied multiplicities determined by DEPT.

than prenylated, non-nitrogenous xanthone derivatives.[2,12] In conclusion, the heterocyclic substitution in compound **2** does not cause a dramatic enhancement in activity. Compound **1**, with an additional hydroxyl group at C-3′ compared to **2**, had a much weaker activity toward *Plasmodium falciparum* (IC_{50} = 3.5 *μ*g/mL).

Compound **3** was active against *Trypanosoma cruzi* (IC_{50} = 1.5 *μ*g/mL) with only a 5-fold decreased potency compared with the reference drug benznidazole (IC_{50} = 0.3 *μ*g/mL). The antiprotozoal activity of **3** is comparable to that published for a series of synthetic chlorinated xanthones carrying aminoalkyl side chains. These compounds were tested, however, only toward *Plasmodium falciparum*, and the best candidate showed an *in vitro* IC_{50} value of 1.4 *μ*g/mL.[10] Thus, in the current study the *in vitro* antiprotozoal activity of xanthones was further substantiated. The substitution of the xanthone nucleus with dioxane/tetrahydropyran moieties, however, does not improve antiprotozoal activity.

Experimental Section

General Experimental Procedures. Optical rotation was measured on a Jasco DIP 140 polarimeter. CD spectra were recorded in CH_3CN on a Jasco J-815 spectropolarimeter in a 1 cm quartz cell at room temperature. The concentration was 60 *μ*g/mL for **1** and 40 *μ*g/mL for **2**. UV and IR spectra were obtained employing Perkin-Elmer Lambda 40 and Perkin-Elmer Spectrum BX instruments, respectively. All NMR spectra were recorded on Bruker Avance 500 DRX or 300 DPX spectrometers in acetone-d_6 or $CDCl_3$. Spectra were referenced to residual solvent signals with resonances at $\delta_{H/C}$ 2.04/29.8 (acetone-d_6) and 7.26/77.0 ($CDCl_3$), respectively. HREIMS were recorded on a Kratos MS 50 spectrometer. ESIMS measurements were recorded employing an API 2000, Applied Biosystems/MDS Sciex. HPLC was carried out using a Merck-Hitachi system equipped with an L-6200A pump, an L-4500A photodiode array detector, a D-6000A interface with D-7000 HSM software, and a Rheodyne 7725i injection system.

Origin of the Algal Sample and Isolation and Taxonomy of the Fungus. The algal species (taxonomy not determined) originated from Kamari on the island Santorini, Greece. Algal samples were processed immediately after collection. The isolation of fungi was carried out using an indirect isolation method. Algal samples were rinsed three times with sterile H_2O. After surface sterilization with 70% EtOH for 15 s the alga was rinsed in sterile artificial seawater (ASW). Subsequently, the alga was aseptically cut into small pieces and placed on agar plates containing isolation medium: 15 g/L agar, ASW 800 mL/L, glucose 1 g/L, peptone from soymeal 0.5 g/L, yeast extract 0.1 g/L, benzyl penicillin 250 mg/L, and streptomycin sulfate 250 mg/L. Fungi growing out of the algal tissue were separated on biomalt medium (biomalt 20 g/L, agar 10 g/L, ASW 800 mL/L) until the culture was pure. The fungal strain 620/GrK 1a isolated from the Greek alga was identified as *Chaetomium* sp. (at the species level). Identification of the fungus was done by Dr. A. W. A. M. de Cock, Centralbureau voor Schimmel Cultures, Utrecht, The Netherlands.

Cultivation. The fungal strain *Chaetomium* sp. was cultivated for 15 weeks on 11 L of solid malt-yeast agar (MYA) medium (4 g/L yeast extract, 10 g/L malt extract, 4 g/L glucose, 15 g/L agar, and ASW, pH 7.3) at room temperature in Fernbach flasks.

Extraction and Isolation. Fungal biomass and media were homogenized using an Ultra-Turrax apparatus and extracted four times with EtOAc. The crude extract (3.5 g) was fractionated using NP-vacuum liquid chromatography (Merck silica gel 60, 63−200 *μ*m, 5.5 × 17 cm) with a petroleum ether/acetone/MeOH gradient, yielding 20

Table 3. 1D and 2D NMR Spectroscopic Data for Chaetoxanthone C (**3**)

atom no.	δ_C[a,c,f]	δ_H[a,c] (mult., *J* in Hz)	COSY[a,d]	HMBC[a,e]	NOESY[a,d]	sel. NOE[b,d]
1	157.2 (C)					
2	109.5 (C)					
3	159.1 (C)					
4	98.3 (C)					
4a	151.0 (C)					
5	110.1 (CH)	7.12 (d, 8.5)	6	7, 8, 8a, 9, 10a	6	
6	135.5 (CH)	7.61 (t, 8.5)	5, 7	5, 7, 8, 8a, 10a	5, 7	
7	106.0 (CH)	6.80 (d, 8.5)	6	5, 8, 8a, 9, 10a	6, 11	
8	160.5 (C)					
8a	110.5 (C)					
9	181.4 (C)					
9a	103.5 (C)					
10a	157.6 (C)					
11	56.5 (CH_3)	4.02 (s)		7, 8	7	
1′	75.8 (CH)	5.14 (dd, 2.1, 11.1)	2′	1, 2, 3, 2′, 3′, 5′	5′	1-OH, 3-OH, 3′α/*β*, 5′
2′	30.3 (CH_2)	1.93 (Hα m)	1′, 3′	4′, 5′		
		1.58 (H*β* m)	1′, 3′	4′, 5′		
3′	23.2 (CH_2)	1.93 (Hα m)	2′, 4′			
		1.73 (H*β* m)	2′, 4′			
4′	33.0 (CH_2)	1.37 (Hα m)	3′, 5′	1′, 2′		
		1.73 (H*β* m)	3′, 5′	1′, 2′		
5′	76.0 (CH)	3.74 (m)	6′	1′, 6′	1′, 6′	1′, 3′*β*
6′	22.1 (CH_3)	1.30 (d, 6.0)	5′	4′, 5′	3-OH, 5′	3-OH, 3′α/*β*, 5′
OH-1		13.62 (s)		1, 2, 3, 9, 9a		
OH-3		10.52 (s)		2, 3, 4, 4a	6′	6′

[a] Chloroform-d_1, 300/75.5 MHz. [b] Chloroform-d_1, 500/125.7 MHz. [c] Assignments are based on extensive 1D and 2D NMR measurements (HMBC, HSQC, COSY). [d] Numbers refer to proton resonances. [e] Numbers refer to carbon resonances. [f] Implied multiplicities determined by DEPT.

Table 4. Antiprotozoal Activities of Compounds **1**−**3**

compd	*T. b. rhod.*[a] IC_{50} (μg/mL)	*T. cruzi*[b] IC_{50} (μg/mL)	*L. don.*[c] IC_{50} (μg/mL)	*P. falc.*[d] IC_{50} (μg/mL)	cytotoxicity[e] IC_{50} (μg/mL)
1	4.7	>10	5.3	3.5	59.1
2	9.3	7.1	3.4	0.5	>90
3	42.6	1.5	3.1	4.0	46.7
ref drug	0.004[f]	0.317[g]	0.125[h]	0.079[i]	0.006[k]

[a] *Trypanosoma brucei rhodesiense* (strain STIB 900). [b] *Trypanosoma cruzi* (strain Tulahuen C4). [c] *Leishmania donovani* (strain MHOM-ET-67/L82). [d] *Plasmodium falciparum* (strain K1). [e] L6-cells. [f] Melarsoprol. [g] Benznidazole. [h] Miltefosine. [i] Chloroquine. [k] Podophyllotoxin.

fractions. Fraction 16 (337 mg) was further fractionated by RP18-VLC (Macherey-Nagel Polygoprep 60−50 C_{18}, 3.2 × 11 cm) with a MeOH/H_2O gradient. Subfraction 3 was then purified via RP18 HPLC (Macherey-Nagel Nucleodur Sphinx RP, 5 μm, 250 × 4.6 mm) with a mobile phase (0.8 mL/min) consisting of 73/27 MeOH/H_2O, resulting in three fractions, of which fraction 2 (16.3.2) afforded the pure compound **1** (6.7 mg). NP-VLC fraction 5 (151 mg) was further fractionated by RP 18 HPLC (Knauer C_{18} Eurosphere 100 250 × 8 mm, 5 μm) with a mobile phase (2.5 mL/min) consisting of 75/25 MeOH/H_2O, resulting in 10 fractions. Of these, subfractions 6 and 9 were processed via RP18 HPLC (Macherey-Nagel Nucleodur Sphinx RP, 5 μm, 250 × 4.6 mm). The purification of subfraction 6 with MeOH/H_2O (80/20) and the flow rate 1.0 mL/min yielded the racemic compound **2** (22.1 mg) in fraction 3 (5.6.3). The second peak of the separation of subfraction 9 (MeOH/H_2O, 85/15, 1.0 mL/min) afforded 8.8 mg of compound **3** (5.9.2).

Modified Mosher Derivatization. Preparation of the Acid Chlorides of (*R*)- and (*S*)-MPA. Oxalyl chloride (103.7 μL, 1.2 mmol) was added to a solution of the corresponding MPA (20 mg, 0.12 mmol) and DMF (0.94 μL, 0.012 mmol) in hexanes at room temperature. After 1 day, the solvent was vacuum-baked to give 100% of the product MPA-Cl (22.2 mg, 0.12 mmol).[25]

Preparation of the (*R*)- and (*S*)-MPA Esters. The corresponding MPA-Cl (5.00 mg, 27.08 μmol) was dissolved in 5 mL of CH_2Cl_2 and added to a solution of compound **1** (2.0 mg, 5.42 μmol), Et_3N (9.01 μL, 64.99 μmol), and DMAP (0.67 mg, 5.42 μmol) as catalyst. After 20 min reaction time the obtained products were dried under vacuum and further purified by HPLC using the Merck-Hitachi system. The separation was performed with a RP18 column (Macherey-Nagel Nucleodur Sphinx RP, 5 μm, 250 × 4.6 mm) and a mobile phase (0.9 mL/min) consisting of MeCN/H_2O, 64/36. The second peak in each chromatogram revealed the pure MPA esters (0.6 mg = 21.4% of *R*-MPA ester and 1.0 mg = 35.6% of *S*-MPA ester, respectively).

Molecular Modeling. All models were calculated employing conformation search (Boltzman jump) and a standard force field as implemented in the Cerius2 4.0 (MSI) molecular modeling software package. Models were further refined with 1500 iterations of minimization. Calculations were performed using a Silicon Graphics O2 workstation (Irix 6.5.6).

Chaetoxanthone A (1): yellow solid (6.7 mg, 0.6 mg/L); $[\alpha]^{24}_D$ −118 (*c* 0.19 $CHCl_3$); UV (MeOH) λ_{max} (log ε) 245 nm (5.52), 323 nm (5.27); IR (ATR) ν_{max} 3499, 1650, 1605, 1478, 1128 cm^{-1}; ^1H and ^{13}C NMR data, see Table 1; ESIMS *m/z* 353 $[M - H_2O + H]^+$; EIMS *m/z* 370 (80), 295 (50), 285 (80), 284 (50), 283 (100), 271 (40); HREIMS *m/z* 370.1059 (calcd for $C_{20}H_{18}O_7$, 370.1053).

Chaetoxanthone B (2): brownish solid (22.1 mg, 2.0 mg/L); $[\alpha]^{24}_D$ +1.7 (*c* 0.15 $CHCl_3$); UV (MeCN) λ_{max} (log ε) 244 nm (4.18), 322 nm (3.90); IR (ATR) ν_{max} 2937, 1644, 1604, 1477, 1247 cm^{-1}; ^1H and ^{13}C NMR data, see Table 2; ESIMS *m/z* 355 $[M + H]^+$; EIMS *m/z* 354 (54), 311 (100), 297 (18), 283 (53); HREIMS *m/z* 354.1100 (calcd for $C_{20}H_{18}O_6$, 354.1103).

Chaetoxanthone C (3): yellow solid (8.8 mg, 0.8 mg/L); $[\alpha]^{24}_D$ +88 (*c* 0.2 $CHCl_3$); UV ($CHCl_3$) λ_{max} (log ε) 265 nm (4.17), 327 nm (4.16); IR (ATR) ν_{max} 2917, 1621, 1592, 1481 cm^{-1}; ^1H and ^{13}C NMR data, see Table 3; ESIMS *m/z* 391 $[M + H]^+$, 389 $[M - H]^-$; EIMS *m/z* 390 (100), 372 (17), 347 (43), 319 (66), 305 (78); HREIMS *m/z* 390.0872 (calcd for $C_{20}H_{19}{}^{35}ClO_6$, 390.0870).

Biological Assays. Pure compounds **1**−**3** were tested in agar diffusion assays[26] against the bacteria *Bacillus megaterium* and *Escherichia coli*, the fungi *Microbotryum violaceum*, *Eurotium rubrum*, and *Mycotypha microspora*, and the green microalga *Chlorella fusca*. Cytotoxicity of the compounds was investigated using 6 or 35 cancer cell line panels.[27,28]

The antiprotozoal activity was determined against the K1 strain of *Plasmodium falciparum*, using a modified [^{3}H]hypoxanthine incorporation assay. The infected human erythrocytes were exposed to serial

drug dilutions in microtiter plates for 48 h at 37 °C in a gas mixture with reduced O_2 and elevated CO_2. [^{3}H]Hypoxanthine was added to each well, and after further incubation for 24 h the wells were harvested on glass fiber filters and counted in a liquid scintillation counter. From the sigmoidal inhibition curve the IC_{50} value was calculated. Chloroquine was used as positive control in each test series. Activity against *Trypanosoma brucei rhodesiense* (strain STIB 900), the causative agent of African sleeping sickness, was evaluated according to Räz et al.[29] Parasites were grown axenically in culture medium supplemented with horse serum. Following a 3-day exposure to compounds **1**, **2**, and **3**, the viability of tryptomastigote parasites was quantified using the dye Almar Blue by monitoring the reductive environment of living cells. Fluorescence development was expressed as percentage of the control, and IC_{50} values were calculated. Melarsoprol was included as positive control. Activity against *Trypanosoma cruzi*, the causative agent of Chagas' disease, was determined according to Buckner et al.[30] Briefly, the strain Tulahuen C4 of *T. cruzi*, which had been transfected with the galactosidase *lac*-Z gene, was cultivated for 4 days on rat skeletal myoblasts (5% CO_2, 37 °C) in the presence of drug. For measurement of the IC_{50} the substrate chlorophenol red-β-D-galactopyranoside was added. The enzyme catalyzed the hydrolysis to the red-colored product that was quantified during the following 2−4 h photometrically employing an ELISA reader. As a positive control, benznidazole was included in each test series. Evaluation of antileishmanial activity was carried out in mouse peritoneal macrophages. The ratio of infection with *Leishmania donovani* (strain MHOM-ET-67/L82), the causative agent of Kala-Azar disease, was determined microscopically after exposure to test compounds, incubation, and staining with Giemsa. IC_{50} values were calculated by linear regression. Miltefosine was used as positive control. An additional reference cytotoxicity assay was evaluated in rat skeletal myoblasts (L6-cells), using podophyllotoxin as positive control.

Acknowledgment. We thank M. Engeser and C. Sondag, University of Bonn, Germany, for recording EIMS spectra, C. Siering, Institute for Organic Chemistry, University of Bonn, Germany, for the CD analyses, and A. Maier as well as H.-H. Fiebig for cytotoxicity assays. For financial support we thank the Bundesministerium für Bildung and Forschung (BMBF), research program 03F0415A.

Supporting Information Available: Key COSY and HMBC correlations, ^{1}H and ^{13}C NMR spectra, as well as the proposed biogenesis of compounds **1**−**3** additional to a figure with related fungal metabolites. Figures with calculated torsion angles, results of modified Mosher's method, and calculated models of **1**. Figures with calculated models of **3**. This material is available free of charge via the Internet at http://pubs.acs.org.

References and Notes

(1) Pinto, M. M. M.; Sousa, M. E.; Nascimento, M. S. J. *Curr. Med. Chem.* **2005**, *12*, 2517–2538.
(2) Molinar-Toribio, E.; González, J.; Ortega-Barría, E.; Capson, T. L.; Coley, P. D.; Kursar, T. A.; McPhail, K.; Cubilla-Rios, L. *Pharm. Biol.* **2006**, *44*, 550–553.
(3) Dua, V. K.; Ojha, V. P.; Roy, R.; Joshi, B. C.; Valecha, N.; Usha Devi, C.; Bhatnagar, M. C.; Sharma, V. P.; Subbarao, S. K. *J. Ethnopharmacol.* **2004**, *95*, 247–251.
(4) Ignatushchenko, M. V.; Winter, R. W.; Riscoe, M. *Am. J. Med. Hyg.* **2000**, *62*, 77–81.
(5) Ridley, R. G. *Nature* **2002**, *415*, 686–693.
(6) Gelb, M. H.; Hol, W. G. J. *Science* **2002**, *297*, 343–344.
(7) Egan, T. J.; Kaschula, C. H. *Curr. Opin. Infect. Dis.* **2007**, *20*, 598–604.
(8) Wu, C.-P.; van Schalkwyk, D. A.; Taylor, D.; Smith, P. J.; Chibale, K. *Int. J. Antimicrob. Agents* **2005**, *26*, 170–175.
(9) Isaka, M.; Jaturapat, A.; Rukseree, K.; Danwisetkanjana, K.; Tanticharoen, M.; Thebtaranonth, Y. *J. Nat. Prod.* **2001**, *64*, 1015–1018.
(10) Portela, C.; Afonso, C. M. M.; Pinto, M. M. M.; Lopes, D.; Nogueira, F.; do Rosário, V. *Chem. Biodiversity* **2007**, *4*, 1508–1519.
(11) Mahabusarakam, W.; Kuaha, K.; Wilairat, P.; Taylor, W. C. *Planta Med.* **2006**, *72*, 912–916.
(12) Hay, A.-E.; Hélesbeux, J.-J.; Duval, O.; Labaïed, M.; Grellier, P.; Richomme, P. *Life Sci.* **2004**, *75*, 3077–3085.
(13) Portela, C.; Afonso, C. M. M.; Pinto, M. M. M.; Ramos, M. J. *Bioorg. Med. Chem.* **2004**, *12*, 3313–3321.
(14) Ignatushchenko, M. V.; Winter, R. W.; Bächinger, H. P.; Hinrichs, D. J.; Riscoe, M. K. *FEBS Lett.* **1997**, *409*, 67–73.
(15) Altona, C. *Encyclopedia Magn. Reson.* **1996**, *8*, 4909–4923.
(16) Seco, J. M.; Quiñoá, E.; Riguera, R. *Chem. Rev.* **2004**, *104*, 17–117.
(17) Maskey, R. P.; Grün-Wollny, I.; Laatsch, H. *J. Antibiot.* **2003**, *56*, 459–463.
(18) Townsend, C. A.; Isomura, Y.; Davis, S. G.; Hodge, J. A. *Tetrahedron* **1989**, *45*, 2263–2276.
(19) O'Malley, G. J.; Murphy, R. A.; Cava, M. P. *J. Org. Chem.* **1985**, *50*, 5533–5537.
(20) Yu, J.; Bhatnagar, D.; Cleveland, T. E. *FEBS Lett.* **2004**, *564*, 126–130.
(21) Bringmann, G.; Noll, T. F.; Gulder, T. A. M.; Grüne, M.; Dreyer, M.; Wilde, C.; Pankewitz, F.; Hilker, M.; Payne, G. D.; Jones, A. L.; Goodfellow, M.; Fiedler, H.-P. *Nat. Chem. Biol.* **2006**, *2*, 429–433.
(22) Gales, L; Damas, A. M. *Curr. Med. Chem.* **2005**, *12*, 2499–2515.
(23) Shimada, A.; Takahashi, I.; Kawano, T.; Kimura, Y. *Z. Naturforsch. B* **2001**, *56*, 797–803.
(24) Kachi, H.; Hattori, H.; Sassa, T. *J. Antibiot.* **1986**, *39*, 164–166.
(25) Ward, D. E.; Rhee, C. K. *Tetrahedron Lett.* **1991**, *32*, 7165–7166.
(26) Schulz, B.; Sucker, J.; Aust, H.-J.; Krohn, K.; Ludewig, K.; Jones, P. G.; Döring, D. *Mycol. Res.* **1995**, *99*, 1007–1015.
(27) Dengler, W. A.; Schulte, J.; Berger, D. P.; Mertelsmann, R.; Fiebig, H.-H. *Anticancer Drugs* **1995**, *6*, 522–532.
(28) Fiebig, H.-H.; Maier, A.; Burger, A. M. *Eur. J. Cancer* **2004**, *40*, 802–820.
(29) Räz, B.; Iten, M.; Grether-Bühler, R.; Kaminsky, R.; Brun, R. *Acta Trop.* **1997**, *68*, 139–147.
(30) Bruckner, F. S.; Verlinde, C. L. M. J.; La Flamme, A. C.; van Voorhis, W. C. *Antimicrob. Agents Chemother.* **1996**, *40*, 2592–2597.

NP800294Q